energies

MDPI

Article

Autonomous DC-Bus Voltage Regulation in DC Microgrid Using Distributed Energy Storage Systems

Jung-Sik Choi, Seung-Yeol Oh, Dae-Seak Cha, Byoung-Sun Ko and Mina Kim *

Intelligent LVDC Demonstration Group, Korea Electronics Technology Institute, Naju-si 58277, Korea; cjs1108@keti.re.kr (J.-S.C.); osy5334@keti.re.kr (S.-Y.O.); dscha@keti.re.kr (D.-S.C.); bsko@keti.re.kr (B.-S.K.)
* Correspondence: minakim@keti.re.kr; Tel.: +82-61-338-4004

Abstract: A DC microgrid has many advantageous features, such as low power losses, zero reactive power, and a simple interface with renewable energy sources (RESs). A bipolar DC microgrid is also highlighted due to its high-power quality, improved reliability, and enhanced system efficiency. However, the bipolar DC microgrid has high DC bus voltage fluctuation due to the load power unbalance between the poles. Therefore, this paper analyzes the DC bus voltage fluctuation that can occur in the bipolar DC microgrid. An autonomous grid voltage regulation method is introduced to regulate the DC bus voltage of a bipolar DC microgrid using distributed energy storage systems (ESSs). The proposed grid voltage regulation scheme using the distributed ESSs could regulate DC bus voltage in real time, regardless of the structure of the DC microgrid without external communication. Lastly, experimental results using a lab-scale bipolar DC microgrid prototype verified the proposed method.

Keywords: bus voltage regulation; DC microgrid; ESS utilization; power distribution system; power management algorithm

check for updates

Citation: Choi, J.-S.; Oh, S.-Y.; Cha, D.-S.; Ko, B.-S.; Kim, M. Autonomous DC-Bus Voltage Regulation in DC Microgrid Using Distributed Energy Storage Systems. *Energies* **2022**, *15*, 4559. https://doi.org/10.3390/en15134559

Academic Editor: Federico Martin Serra

Received: 18 May 2022
Accepted: 18 June 2022
Published: 22 June 2022

Publisher's Note: MDPI stays neutral with regard to jurisdictional claims in published maps and institutional affiliations.

Copyright: © 2022 by the authors. Licensee MDPI, Basel, Switzerland. This article is an open access article distributed under the terms and conditions of the Creative Commons Attribution (CC BY) license (https://creativecommons.org/licenses/by/4.0/).

1. Introduction

DC microgrids can achieve low power losses, zero reactive power, and uncomplicated power interfaces with renewable energy sources (RESs) [1,2]. The power converters that construct DC microgrids can achieve high dynamic performance with superior voltage and current regulation capability. Therefore, DC microgrids have rapid fault-current limitation and propagation rejection capabilities. Consequently, compared to conventional AC grids, DC microgrids can obtain higher-power distribution efficiency, reliability, and sustainability [3].

A bipolar DC microgrid is highlighted since it can improve system efficiency, power quality, and reliability [4–7]. Figure 1 shows the structure of a bipolar DC microgrid. It offers high reliability, since a pole continuously supplies power even when the other pole fails to operate. A multilevel AC/DC converter can interface the bipolar DC microgrid with the AC grid with a single converter. However, the multilevel AC/DC converter has a voltage unbalance between the poles when the load power of each pole is not balanced. This brings low reliability to the DC microgrid, high voltage stress applied to the components, and a short lifetime for power converters. Consequently, a DC bus voltage regulation method that can operate in a bipolar DC microgrid is required to preserve the stable operation of the DC microgrid.

There are several previous DC bus regulation methods for DC microgrids. A central controller can mainly regulate DC bus voltage by controlling the current of the ESS and AC/DC converter [8]. However, the central controller may destroy the reliability of the DC microgrid when it fails to operate and control the DC bus voltage. A droop control can also be utilized to regulate the DC bus voltage of DC microgrids [9–11]. However, it is vulnerable to transmission line impedance and brings DC bus voltage fluctuations. The

droop control could also minimize the DC bus voltage fluctuation, but it requires communication with the neighboring circuits. There are several DC bus regulation algorithms for DC microgrids, including time- or event-triggered controls, consensus strategies, and hierarchical control [12–18]. However, they require a communication network among the circuit components, and power converters across the entire DC microgrid. They also cannot successfully regulate sudden local under- and overvoltage conditions due to their long communication delay, assuming a large DC microgrid. Lastly, DC bus regulation methods that utilize PV panels and ESSs were introduced [19–21]. The DC bus voltage regulation shown in [19] can regulate DC bus voltage and perform maximal power point tracking (MPPT) for PV panels. However, it can only deal with a constant load condition. The DC bus regulation scheme shown in [20] analyzed distributed ESSs in a DC microgrid that could reduce the DC bus voltage drop due to transmission line impedance. However, the authors in [20] did not provide a detailed implementation of the ESSs, such as the power interface of the ESSs, the charging and discharging strategy, and load variant conditions. The DC bus voltage regulation strategy shown in [21] also utilized distributed ESSs to overcome the overvoltage condition due to the high penetration of PV power generation. It introduced an ESS charging scheme along with PV power generation; therefore, it could successfully deal with sudden overvoltage conditions due to PVs. However, it cannot regulate the undervoltage conditions of DC microgrids.

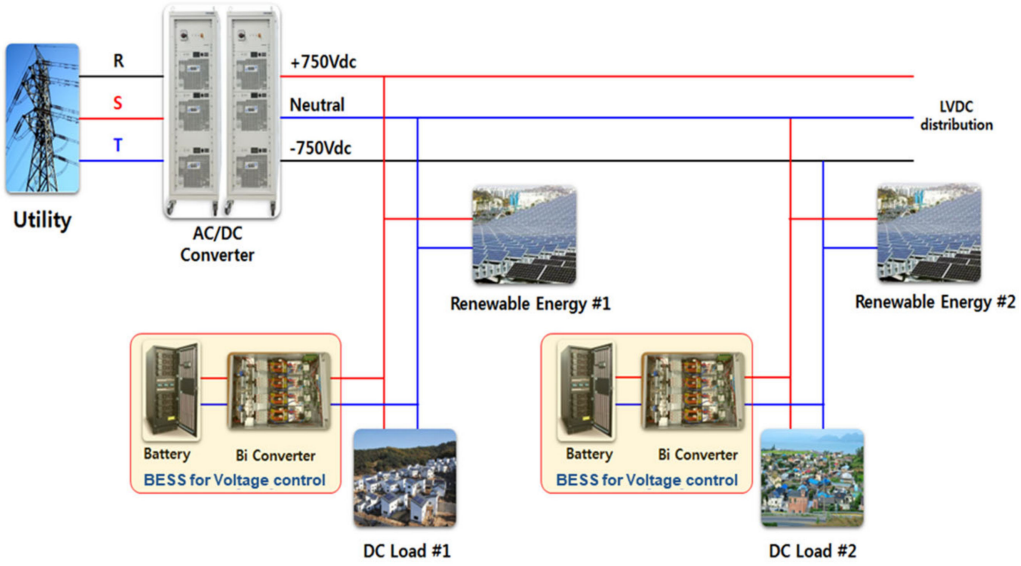


Figure 1. Overall structure of bipolar DC microgrid.

In this paper, an effective DC bus voltage regulation method is proposed for bipolar DC microgrids. The DC bus voltage fluctuation of bipolar DC microgrids is comprehensively discussed. An autonomous grid voltage regulation method is also proposed to regulate the DC bus voltage of a bipolar DC microgrid. Since a bipolar DC microgrid cannot freely adopt conventional DC bus regulation methods, distributed ESSs installed at the end side were utilized. Distributed ESSs with a bidirectional power interface continuously monitor the DC bus voltage of the end sides. When the DC bus voltage of the end sides experiences an under- or overvoltage condition, the bidirectional power interfaces start to charge or discharge the distributed ESSs to regulate the DC bus voltage of the end sides. Therefore, the proposed algorithm can control the DC bus voltage of the end sides in real time without additional communication with the neighboring circuits or converters, and complex load and power generation estimation algorithms. This method can minimize the configuration of a DC microgrid, and maximize its cost-effectiveness and reliability. It can also be freely adopted by any DC microgrid regardless of its structure. Lastly, the proposed method was validated through experimental results using a lab-scale bipolar DC microgrid prototype.

2. DC Bus Voltage Analysis in Bipolar DC Microgrid

Although the AC/DC converter that interfaces the DC microgrid and AC grid regulates DC bus voltage, the DC bus voltage of the DC microgrid can suffer from severe under- and overvoltage fault conditions. In this section, the under- and overvoltage conditions of bipolar DC bus voltage are analyzed.

2.1. Limited Power Capacity of AC/DC Converter

Over- and undervoltage fault conditions can occur due to the limited power capacity of the central AC/DC converter and unintentional high-power generation from RESs. Figure 2a shows the overvoltage condition of a DC microgrid. When RESs generate high power while power consumption from the load is low, the central AC/DC converter cannot regulate the DC bus voltage due to the limited current absorbing capacity. On the other hand, undervoltage conditions can occur due to high load consumption and high transmission line impedance. Figure 2b shows the undervoltage condition of a DC microgrid. The transmission line had proportional resistive impedance to the length of the transmission line. As the impedance of the transmission line and the load current increase, the DC bus voltage on the load side decreases, which may cause an undervoltage fault in DC microgrids. In the next subsection, the undervoltage fault of DC microgrids is numerically analyzed.

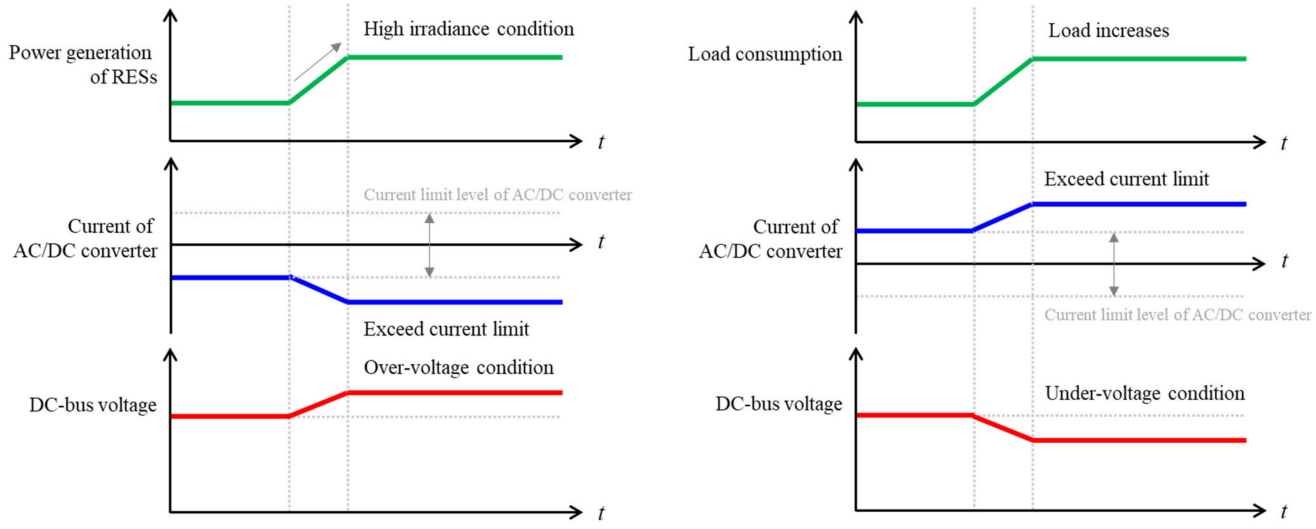


Figure 2. Over- and undervoltage fault conditions of DC bus voltage in DC microgrids: (**a**) Overvoltage fault condition, (**b**) Under-voltage fault condition.

2.2. Transmission Line Impedance

Figure 3 is the impedance diagram of a simplified DC microgrid to analyze the voltage drop due to transmission line impedance and load consumption, where V_{cmd} is the nominal voltage of the DC bus, V_{load} is the DC bus voltage at the end side, K is the DC bus voltage maintenance ratio at the end side, R is the normalized transmission line impedance (Ω/km), D_l is the length of the transmission line, and I_{DC} is the current flowing through the DC bus. Using Figure 3, the DC bus voltage and the power at the end side can be derived as follows:

$$V_{load} = V_{cmd} - (RD_l)I_{DC} \geq KV_{cmd} \tag{1}$$

$$P_{load} = V_{load}I_{DC} = \{V_{cmd} - (RD_l)I_{DC}\}I_{DC} \tag{2}$$

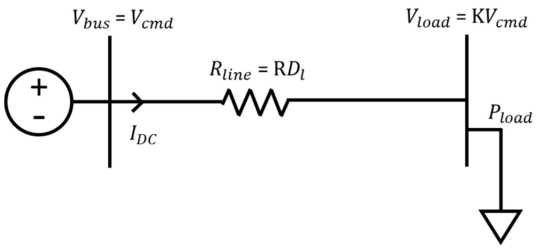


Figure 3. Impedance diagram of a simplified DC microgrid.

On the basis of Equations (1) and (2), the available length of the transmission line to maintain the desired voltage maintenance ratio can be expressed as follows:

$$D_l \leq \frac{K(1-K){V_{cmd}}^2}{P_{load}R} \tag{3}$$

Equation (3) implies that the available length of the transmission line decreases as the load power and the normalized transmission line impedance increase, and the nominal DC bus voltage decreases. However, a transmission line that has low normalized impedance is expensive. Therefore, it is hard to find a proper solution that preserves the DC bus voltage of a DC microgrid with a reasonable power rating and construction cost. Figure 4 shows the calculation results of the available length of the transmission line according to the load power. The available transmission line length for a reasonable voltage maintenance ratio decreases as the load increases. The available transmission line length is 23.10 km when the load power is 100 kW, while it is only 4.62 km when the load power is 500 kW. In other words, a DC microgrid with a high-power rating must be constructed within a small physical dimension to preserve a reasonable voltage maintenance ratio. However, solutions drawn in this analysis such as limited power capacity, expensive transmission lines, and small physical dimensions are not practical. Consequently, a DC microgrid requires the DC bus voltage regulation method as the power rating increases.

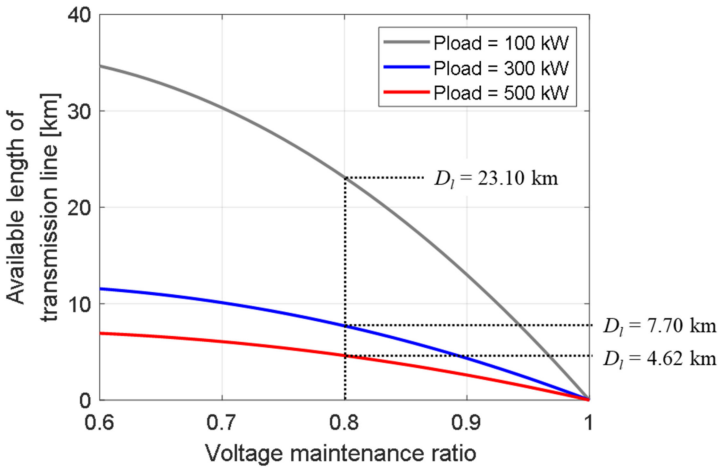


Figure 4. Available length of the transmission line according to the load power.

2.3. Load Unbalance between Poles

A bipolar DC microgrid requires an AC/DC converter that can provide the bipolar output voltage. Figure 5 shows the power stage configuration of a three-level neutral-point clamped (NPC) converter that can provide the bipolar output voltage (V_{po}, V_{on}) with a single converter. However, the bipolar output voltage is very vulnerable to the load unbalance. Figure 6a shows the PSIM simulation results of the three-level NPC converter with load unbalance between the poles. The three-level NPC converter had proportional voltage unbalance to the load unbalance. It could also not provide the acceptable bal-

anced output voltage when the load unbalance was higher than 10%. The three-level NPC converter can compensate the voltage unbalance between the poles using additional control algorithms [22–24]. Figure 6b shows the simulation results of a three-level NPC converter with the load unbalance and voltage unbalance control algorithm. Although the voltage unbalance algorithm compensates the DC components of the voltage unbalance, the AC components of the voltage unbalance are kept. The AC components of the voltage unbalance were also proportional to the load unbalance. Since it induces the high peak of the DC bus voltage, it increases the voltage stress, and brings the low reliability and lifetime of the power converters into the DC microgrid.

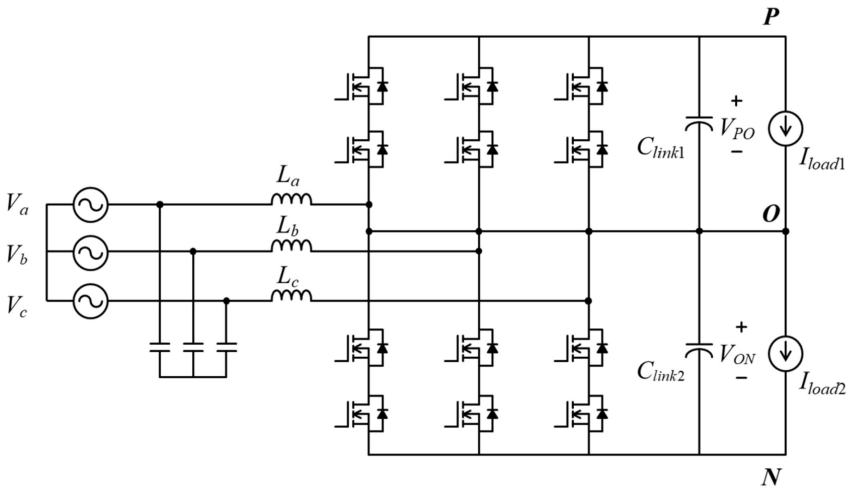
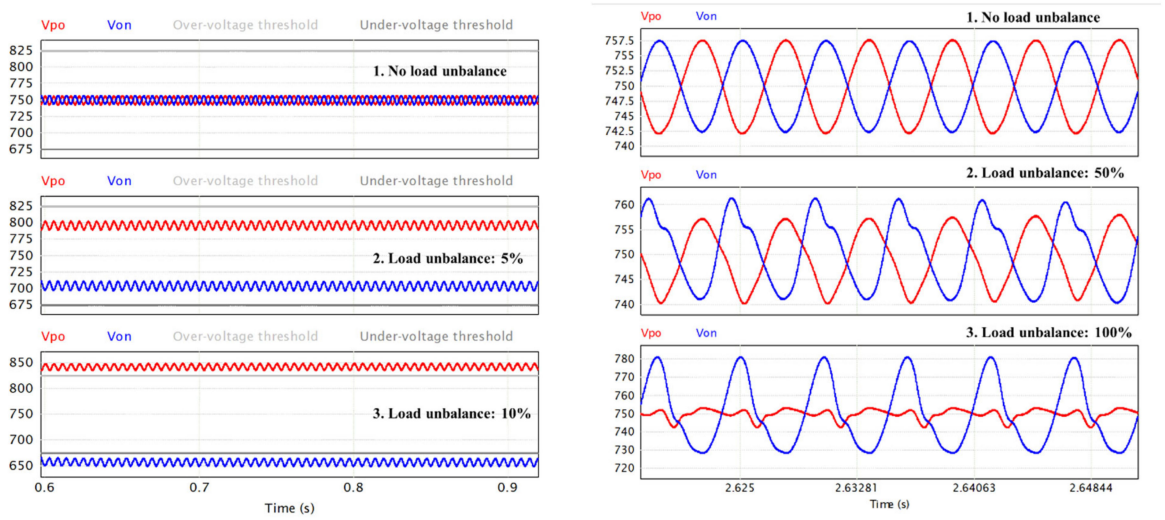


Figure 5. Power stage configuration of three-level NPC converter.



(**a**) (**b**)

Figure 6. PSIM simulation results of three-level NPC converter with unbalanced load: (**a**) without voltage unbalance compensation algorithm, (**b**) with voltage unbalance compensation algorithm.

From the DC bus voltage analysis of the bipolar DC microgrid, the high penetration of the RESs, transmission line impedance, and the low tolerance of the multilevel AC/DC converter according to the load unbalance cause the DC bus voltage fluctuation. Therefore, the proposed DC bus regulation method utilizes Ω distributed ESSs as the energy buffer to minimize the load unbalance of each pole. The detailed DC bus regulation method using distributed ESSs is presented in the next section.

3. Autonomous DC Bus Voltage Regulation Algorithm

3.1. Bidirectional Power Interface for Distributed ESS

Figure 7 shows the bidirectional power interface for distributed ESSs in a DC microgrid. The bidirectional power interface consisted of a four-legged interleaved bidirectional half-bridge topology. Each leg of the bidirectional power interface had a 90° phase shift to suppress the input current ripple, and the voltage and current stress applied to the components. Due to the phase shift of each leg, the bidirectional power interface could reduce the required output capacitance due to the four times increased effective switching frequency [25]. The bidirectional power interface charges or discharges the distributed ESSs on the basis of the current reference determined by the proposed DC bus voltage regulation algorithm. Specifically, the bidirectional power interface controls the entire input current and the input currents of each leg to evenly share the current regardless of the different tolerance levels of the components.

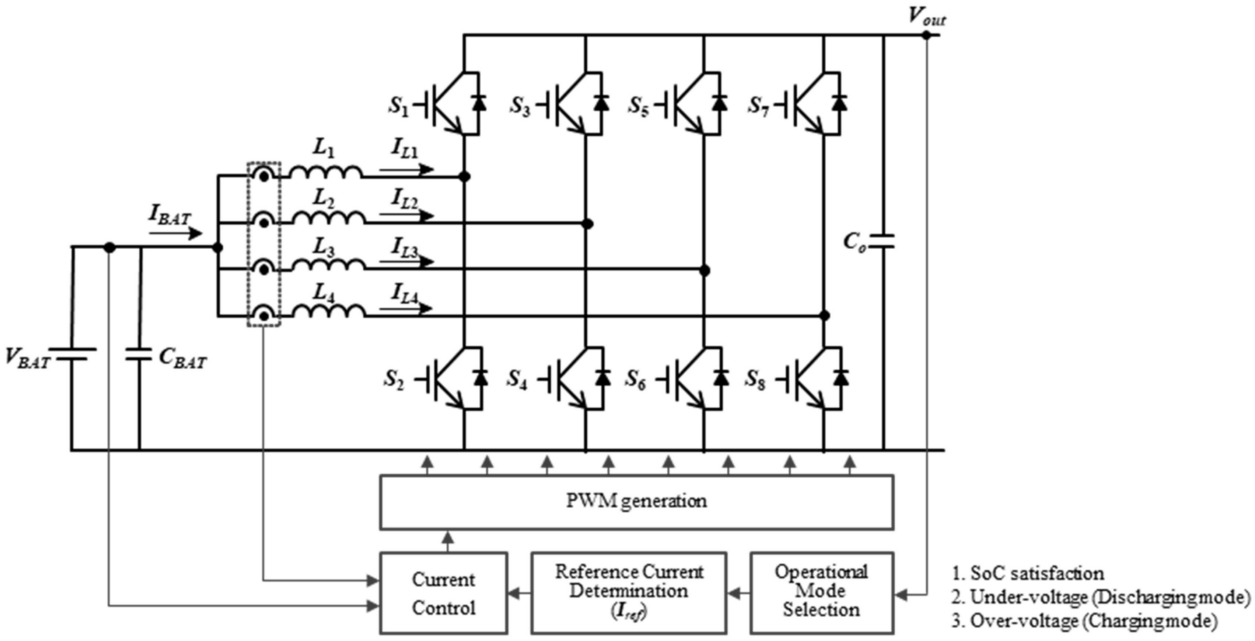


Figure 7. Bidirectional power interface for distributed ESS.

3.2. DC Bus Voltage Regulation Principles

Distributed ESSs in a DC microgrid perform in two operating modes: an islanding mode and a voltage regulation mode. The islanding mode of distributed ESSs generates the DC bus voltage to maintain the normal operating condition of the DC microgrid without an AC grid connection. The voltage regulation mode of distributed ESSs operates when the DC microgrid connects with the AC grid. In this condition, the bidirectional power interfaces of the distributed ESSs continuously monitor the DC bus voltage at the end side. When the DC bus voltage at the end side increases or decreases, the corresponding bidirectional power interface charges or discharges the distributed ESSs to recover the DC bus voltage at the end side as a normal value. In these sequences, the distributed ESSs can balance the load current unbalance between each pole indirectly. When the DC bus voltage of the end side is under abnormal fault conditions, the corresponding bidirectional power interface disconnects the distributed ESSs with the DC bus. These sequences do not require communication with the central controller or neighboring circuits. In this section, the voltage regulation mode of distribution ESSs is specifically discussed.

Figure 8 shows a prior state-of-charge (SoC) satisfaction algorithm. This mode is required to charge and discharge ESSs in preparation for the voltage regulation mode.

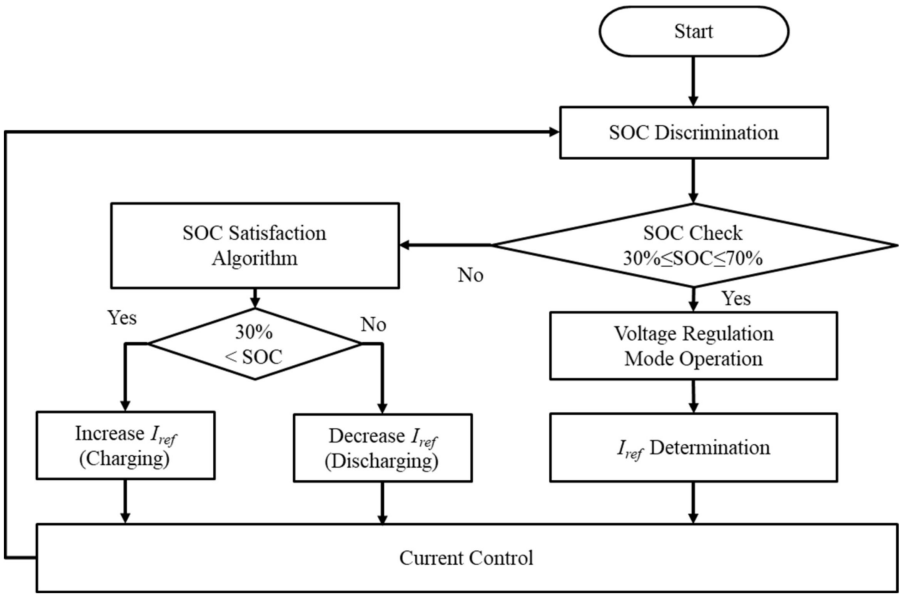


Figure 8. Prior SoC satisfaction algorithms of the distributed ESSs.

The bidirectional power interfaces of distributed ESSs communicate with the battery management system (BMS) of the distributed ESSs to estimate the SoC and current state of the battery. If the SoC of the battery exceeds the range for the voltage regulation mode, the bidirectional power interfaces charge or discharge the battery to meet the SoC range for the voltage regulation mode.

Figure 9 shows the detailed voltage regulation mode to regulate the DC bus voltage of end sides. The bidirectional power interface continuously monitors the DC bus voltage for a preset interval to measure the DC bus voltage in a steady state. In this paper, assuming that the crossover frequency of the AC/DC converter was 100 Hz, the monitoring interval was set to be 10 ms. The normal DC bus voltage range is within ±4% of the nominal DC bus voltage, and the fault thresholds of the DC bus voltage are ±10% of the nominal DC bus voltage. When over- or undervoltage fault conditions occur, the entire DC microgrid stops operating. Therefore, when the DC bus voltage is from ±4% to ±10% of the nominal value of the nominal DC bus voltage, the distributed ESSs recognize the over- or undervoltage conditions and operate the voltage regulation mode.

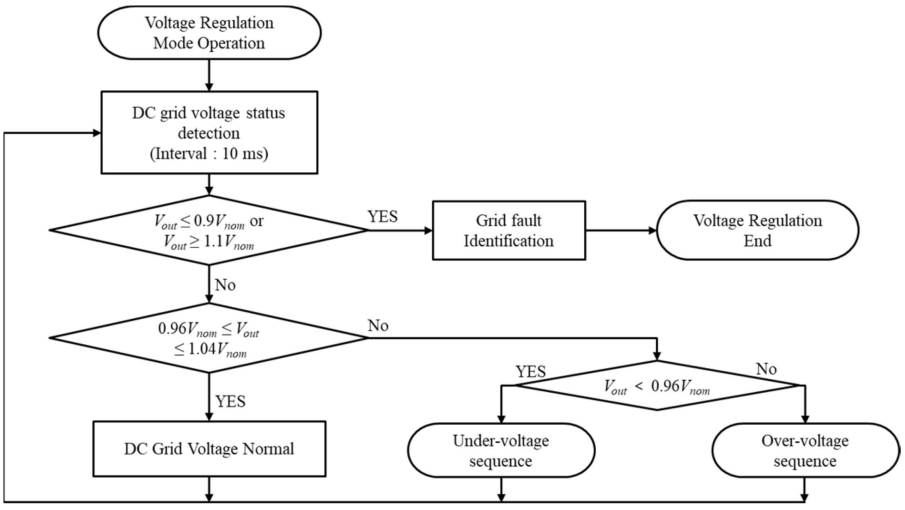


Figure 9. Flowchart of voltage regulation mode.

Figure 10 shows the charging and discharging sequences of the voltage regulation mode at under- and overvoltage conditions. When the bidirectional power interface detects an under- or overvoltage condition, it charges or discharges the distributed ESS with a gradually increased reference current. When the DC bus voltage recovers its normal voltage range, the bidirectional power interface gradually decreases the charging or discharging current after 10 s as the stabilization time. If the DC bus voltage can maintain a normal voltage range after the current of the bidirectional power interface becomes zero, the bidirectional power interface completes the voltage regulation mode. However, if not, the bidirectional power interface restarts the sequence discussed above.

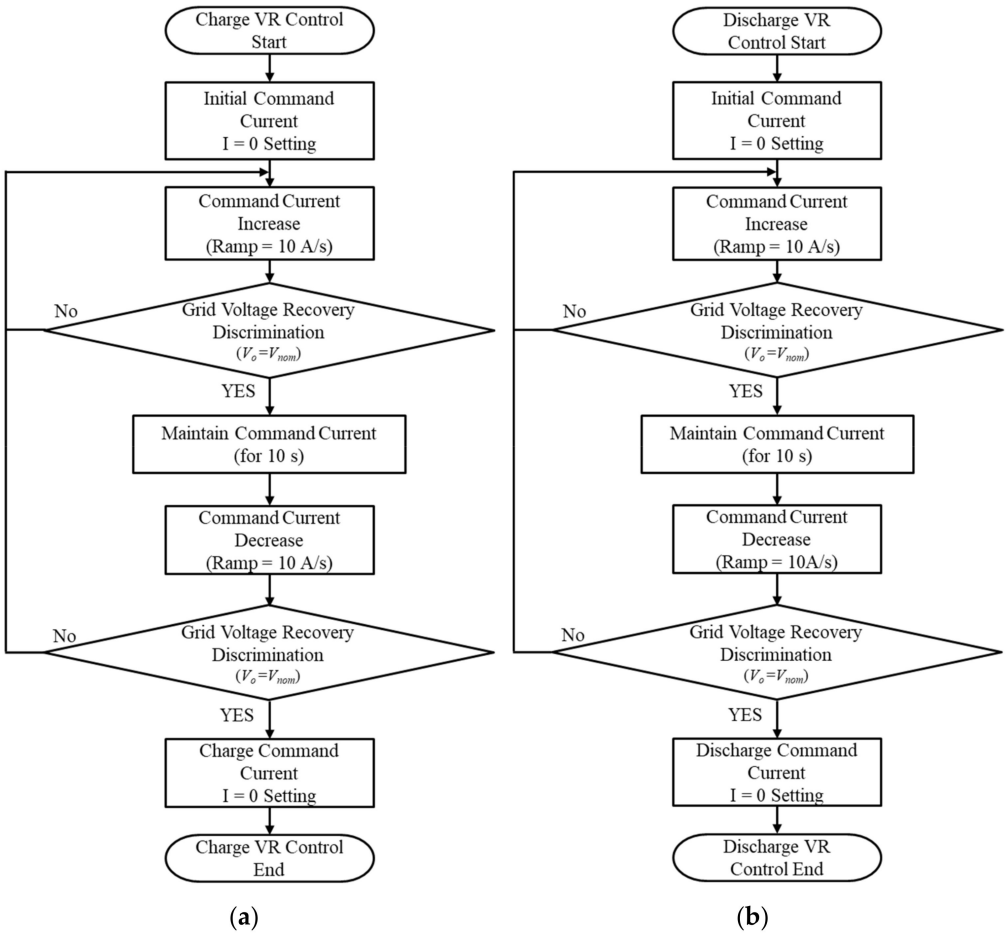
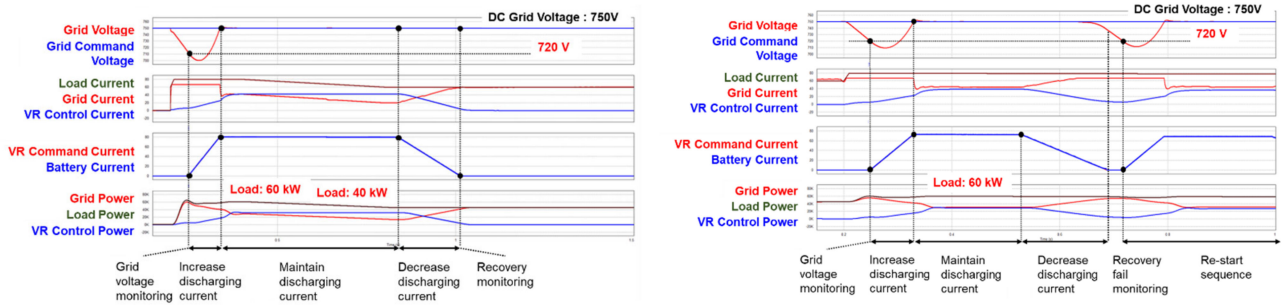


Figure 10. Flowchart of DC bus voltage regulation: (**a**) under- and (**b**) overvoltage sequences.

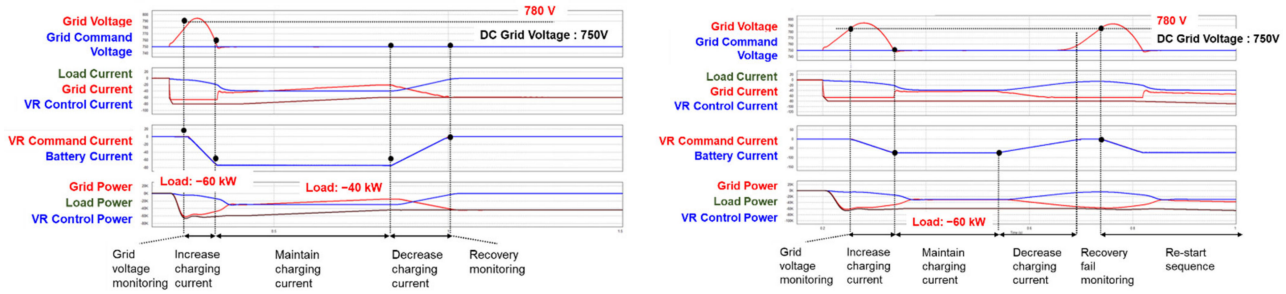
Figure 11a shows the simulation results of the proposed voltage regulation algorithm at an undervoltage condition due to high transmission line impedance and sudden peak load. When the DC bus voltage decreases by 4% of its nominal value, the bidirectional power interface of the ESSs monitors the DC bus voltage for 10 ms to check the steady-state DC bus voltage. If the DC bus voltage does not exceed the fault threshold, the bidirectional power interface starts to discharge the ESS and control the DC bus voltage. As the bidirectional power interface discharges the ESS, the DC bus voltage can recover its nominal value. When the bidirectional power interface detects the DC bus voltage recovery, it starts to reduce the discharging current. If the DC bus voltage does not recover its nominal voltage when the discharging current decreases, the bidirectional power interface restarts the algorithm to recover the DC bus voltage as shown in Figure 11b.



(**a**) (**b**)

Figure 11. Simulation results of the proposed DC bus voltage regulation method at undervoltage condition: (**a**) when peak load is successfully eliminated; (**b**) when peak load is not eliminated.

Figure 12a shows the simulation results of the proposed voltage regulation algorithm at the overvoltage condition due to the high-power generation of RESs. Similar to the undervoltage condition, when the DC bus voltage increases by 4% of its nominal value, the bidirectional power interface monitors the DC bus voltage with an interval of 10 ms. If the DC bus voltage is not higher than the fault threshold, the bidirectional power interface starts to charge the ESS and control the DC bus voltage. The detailed sequence at the overvoltage condition is the same as that in the undervoltage condition. As shown in the simulation results, the proposed grid voltage regulation method could preserve stable DC bus voltage even though there were high transmission line impedance, sudden peak load, and intentional high-power generation from the RESs.



(**a**) (**b**)

Figure 12. Simulation results of the proposed DC bus voltage regulation method at overvoltage condition: (**a**) when high power generation is successfully eliminated; (**b**) when high power generation is not eliminated.

4. Experimental Verifications

Figure 13 and Table 1 show the lab-scale DC microgrid prototype to verify the feasibility of the proposed grid voltage regulation algorithm. The DC microgrid prototype consists of a bidirectional grid voltage simulator to emulate the DC bus voltage, a PV simulator, and a battery with a four-legged interleaved bidirectional power interface. Figure 14 shows the experimental results of the proposed DC bus voltage regulation method at the undervoltage condition. During the monitoring interval (10 ms), the bidirectional power interface could recognize the undervoltage condition. Therefore, the bidirectional power interface start increasing the discharging current. When the DC bus voltage recovers the nominal value as discharge of the distributed ESS, the bidirectional power interface holds the discharging current for stabilization. Since the DC bus voltage drops again after the discharging current is eliminated, the bidirectional power interface restarts the discharging sequence. The sequence could also deal with additional voltage drop due to the additional peak load during bidirectional power interface discharges, as shown in Figure 15. When the DC bus voltage drops during the sequence, the bidirectional power interface increases

the discharging current with a predetermined ramp slope (10 A/s) to recover the DC bus voltage. Lastly, when the DC bus voltage successfully recovers its nominal value, the proposed voltage regulation algorithm at undervoltage conditions completes the sequence as shown in Figure 16.

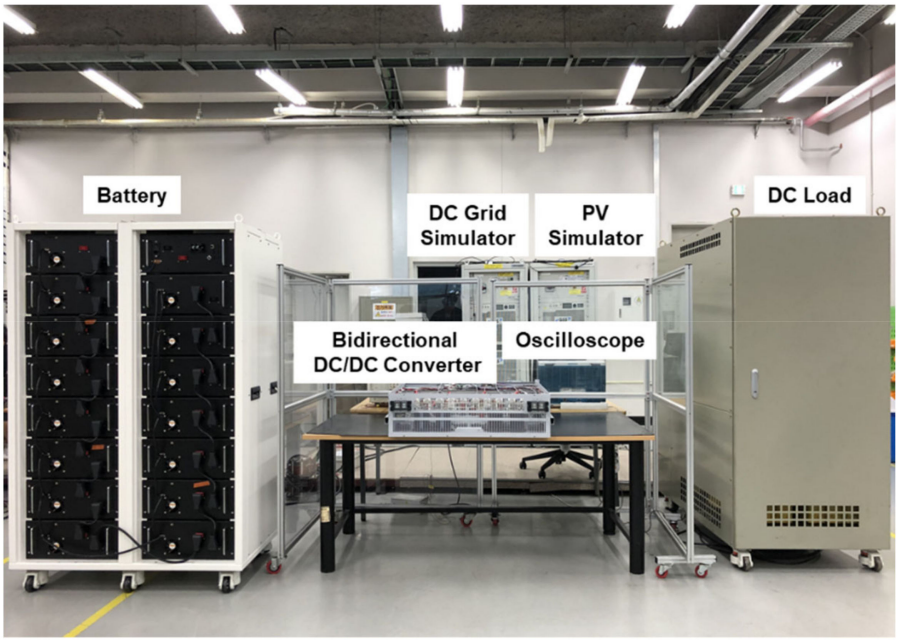


Figure 13. Experimental setup of lab-scale DC microgrid prototype.

Table 1. Hardware configurations of lab-scale DC microgrid prototype.

Components	Value
Battery	50 kWh
Bidirectional power interface	25 kW
PV simulator	60 kW
DC grid simulator	50 kW
DC load	60 kW

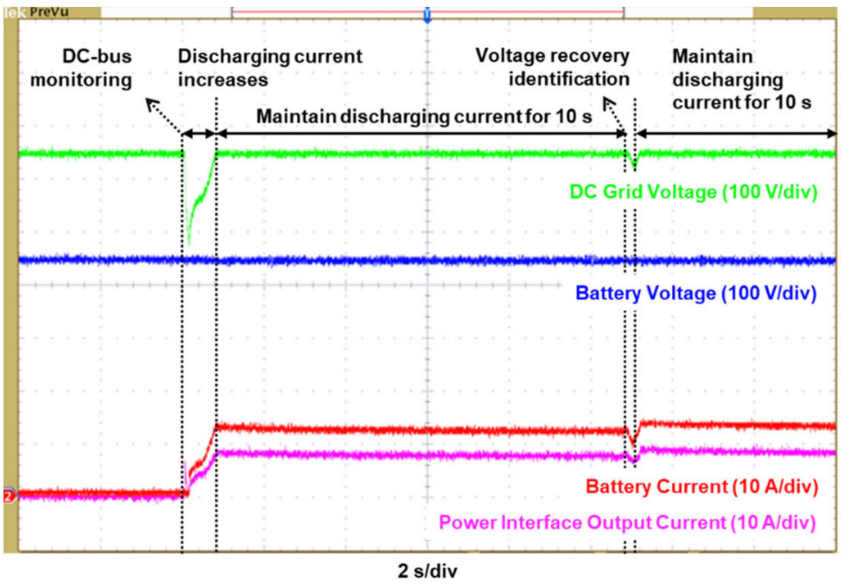


Figure 14. Experimental results of proposed voltage regulation algorithm at undervoltage condition.

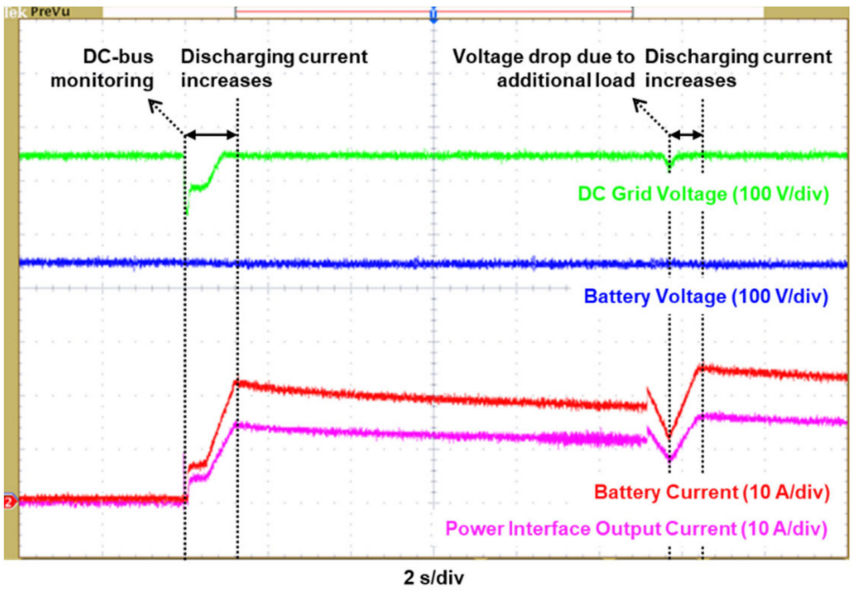


Figure 15. Experimental results of proposed voltage regulation algorithm at undervoltage condition with additional peak load.

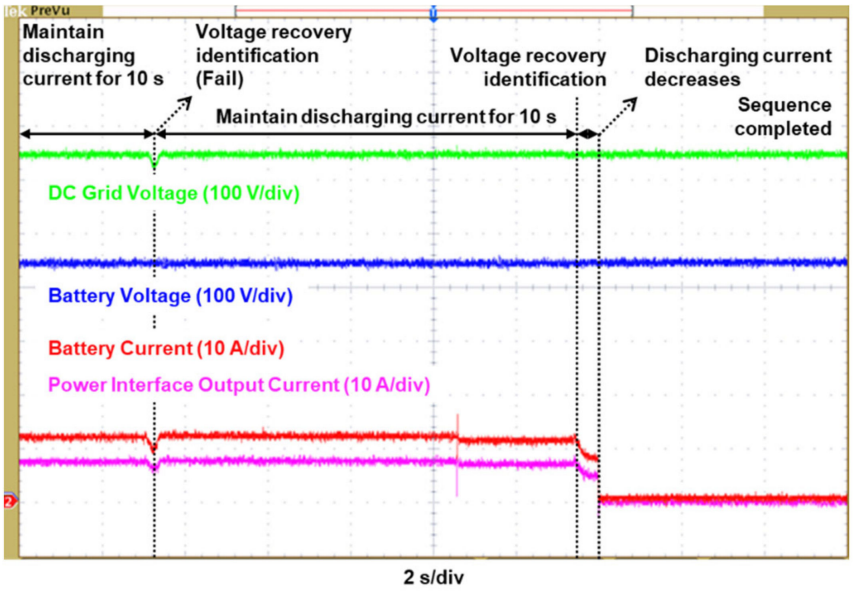


Figure 16. Completion sequence of proposed voltage regulation algorithm at undervoltage condition.

Figure 17 shows the experimental results of the proposed DC bus voltage regulation method at the overvoltage condition. Similar to the undervoltage condition, the bidirectional power interface recognizes the overvoltage condition of the DC bus during the monitoring interval. In that case, the bidirectional power interface starts increasing the charging current. When the DC bus voltage recovers the nominal value, the bidirectional power interface holds the charging current for 10 s. Since the DC bus voltage increases again after the charging current is eliminated, the bidirectional power interface restarts the charging sequence again. Lastly, when the DC bus voltage successfully recovers its nominal value, the proposed voltage regulation algorithm at overvoltage condition completes the sequence as shown in Figure 18.

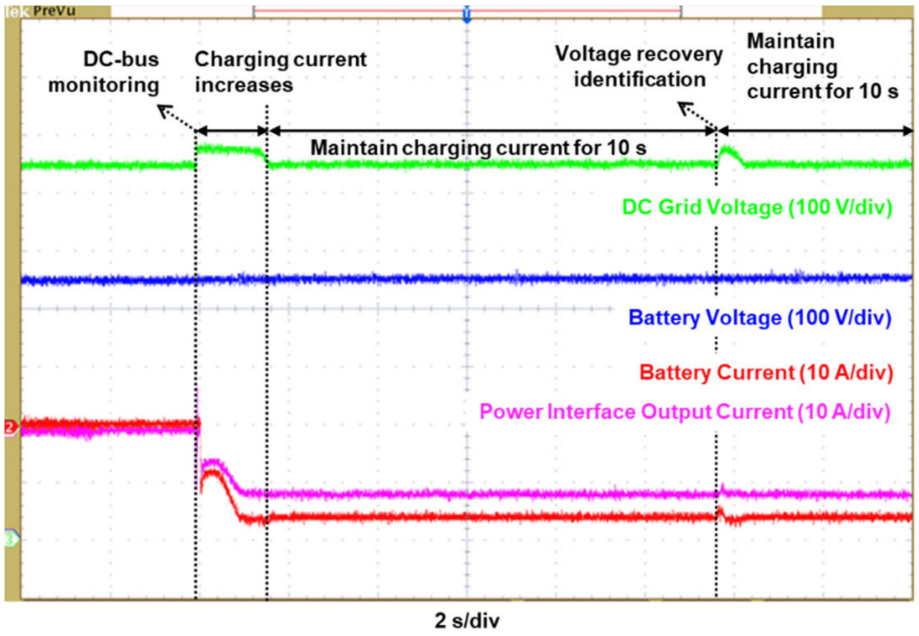


Figure 17. Experimental results of proposed voltage regulation algorithm at overvoltage condition.

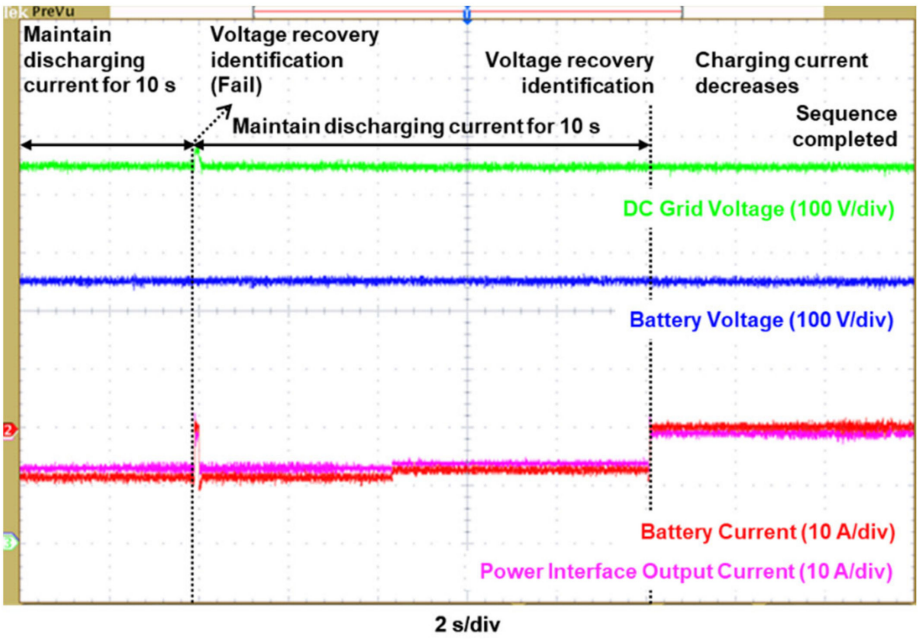


Figure 18. Completion sequence of proposed voltage regulation algorithm at overvoltage condition.

Figures 19 and 20 show the proposed voltage regulation algorithm at fault conditions. Although the charging or discharging sequence operates, the bidirectional power interface can simultaneously deal with fault conditions. When the DC bus voltage exceeds the fault thresholds, the proposed voltage regulation algorithm can successfully distinguish the fault conditions of the DC bus and safely disconnect the ESS with the DC bus to reject the failure propagation.

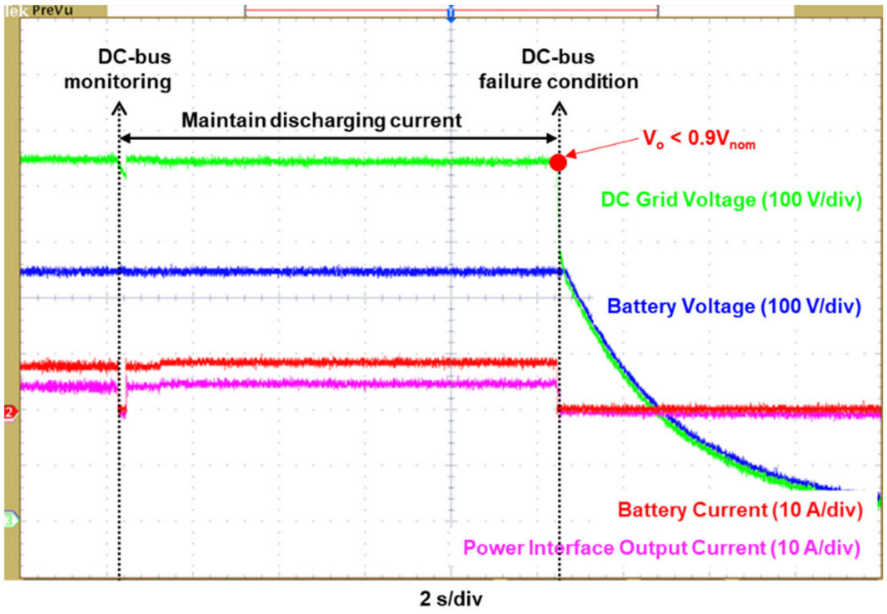


Figure 19. Fault response of proposed voltage regulation algorithm in charging sequence.

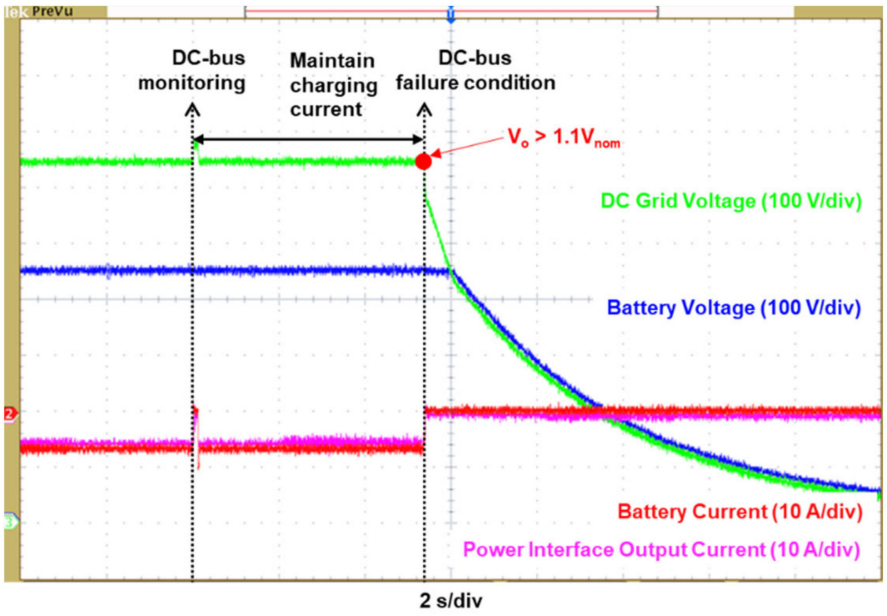


Figure 20. Fault response of proposed voltage regulation algorithm in discharging sequence.

5. Conclusions

In this paper, the DC bus voltage deviation of bipolar DC microgrids was addressed. A bipolar DC microgrid may have DC bus voltage deviations due to practical transmission line impedance, the unpredictable power generation of the RESs, and the unbalanced load of each pole. Since a bipolar DC microgrid requires balanced load power and tightly regulated DC bus voltage, an autonomous DC bus voltage regulation algorithm was presented using the distributed ESSs. The proposed DC bus voltage regulation method can effectively suppress high voltage fluctuation by charging and discharging the distributed ESSs implemented at the end sides. It can regulate the DC bus voltage without additional communication with the neighboring circuit and algorithm by charging and discharging sequences of the distributed ESSs. It can also manage the under- and overvoltage conditions of the DC bus voltage, and successfully disconnect and protect distribution ESSs at fault

conditions. The effectiveness of the proposed voltage regulation method was validated by simulation and experimental results using a lab-scale DC microgrid.

The proposed DC bus voltage regulation method was qualitatively discussed in this paper, focusing on the concept that regulates the DC bus voltage of bipolar DC microgrids. However, quantitative analysis is also required to obtain the proper capacity of the distributed ESSs, the power rating and dynamic performance of the power interface, and the unit load for single distributed ESSs. Our future research will address the quantitative analysis to obtain a general design guideline of the proposed method.

Author Contributions: Conceptualization, J.-S.C.; methodology, D.-S.C.; software, J.-S.C.; validation, D.-S.C. and J.-S.C.; formal analysis, B.-S.K.; investigation, S.-Y.O.; resources, S.-Y.O.; data curation, M.K.; writing—original draft preparation, S.-Y.O.; writing—review and editing, M.K.; visualization, B.-S.K.; supervision, M.K.; project administration, S.-Y.O.; funding acquisition, S.-Y.O. All authors have read and agreed to the published version of the manuscript.

Funding: This work was supported by the Korea Institute of Energy Technology Evaluation and Planning (KETEP) and the Ministry of Trade, Industry, and Energy (MOTIE) of the Republic of Korea (no. 20193810100010).

Institutional Review Board Statement: Not applicable.

Conflicts of Interest: The authors declare no conflict of interest.

References

1. Li, X.; Hui, D.; Lai, X. Battery Energy Storage Station (BESS)-Based Smoothing Control of Photovoltaic (PV) and Wind Power Generation Fluctuations. *IEEE Trans. Sustain. Energy* **2013**, *4*, 464–473. [CrossRef]
2. Vrettos, E.; Papathanassiou, S. Operating Policy and Optimal Sizing of a High Penetration RES-BESS System for Small Isolated Grids. *IEEE Trans. Energy Convers.* **2011**, *26*, 744–756. [CrossRef]
3. Rodriguez-Diaz, E.; Savaghebi, M.; Vasquez, J.C.; Guerrero, J.M. An overview of low voltage DC distribution systems for residential applications. In Proceedings of the 2015 IEEE 5th International Conference on Consumer Electronics—Berlin (ICCE-Berlin), Berlin, Germany, 6–9 September 2015.
4. Kakigano, H.; Miura, Y.; Ise, T. Low-voltage bipolar-type DC microgrid for Super High Quality Distribution. *IEEE Trans. Power Electron.* **2010**, *25*, 3066–3075. [CrossRef]
5. Prabhakaran, P.; Agarwal, V. Novel Four-port DC–DC converter for interfacing solar PV–fuel cell hybrid sources with low-voltage bipolar DC microgrids. *IEEE J. Emerg. Sel. Top. Power Electron.* **2020**, *8*, 1330–1340. [CrossRef]
6. Broeck, G.V.; Martinez, W.; Dalla Vecchia, M.; Ravyts, S.; Driesen, J. Conversion efficiency of the buck three-level DC–DC converter in unbalanced bipolar DC microgrids. *IEEE Trans. Power Electron.* **2020**, *35*, 9306–9319. [CrossRef]
7. Chapparya, V.; Singh, S.P.; Dey, A. Novel non-isolated boost-zeta interleaved DC-DC converter for low voltage bipolar DC Microgrid application. In Proceedings of the 2022 IEEE International Conference on Power Electronics, Smart Grid, and Renewable Energy (PESGRE), Trivandrum, India, 2–5 January 2022.
8. Wu, T.-F.; Chang, C.-H.; Lin, L.-C.; Chang, Y.-C. DC-bus voltage control for three-phase bi-directional inverter in DC microgrid applications. In Proceedings of the 2012 Twenty-Seventh Annual IEEE Applied Power Electronics Conference and Exposition (APEC), Orlando, FL, USA, 5–9 February 2012.
9. Guerrero, J.M.; Vasquez, J.C.; Matas, J.; de Vicuna, L.G.; Castilla, M. Hierarchical Control of Droop-Controlled AC and DC Microgrids—A General Approach Toward Standardization. *IEEE Trans. Ind. Electron.* **2011**, *58*, 158–172. [CrossRef]
10. Ito, Y.; Zhongqing, Y.; Akagi, H. DC microgrid based distribution power generation system. In Proceedings of the 4th International Power Electronics and Motion Control Conference, Xi'an, China, 14–16 August 2004.
11. Khorsandi, A.; Ashourloo, M.; Mokhtari, H. An adaptive droop control method for low voltage DC microgrids. In Proceedings of the 5th Annual International Power Electronics, Drive Systems and Technologies Conference (PEDSTC 2014), Tehran, Iran, 5–6 February 2014.
12. Fan, B.; Peng, J.; Yang, Q.; Liu, W. Distributed periodic event-triggered algorithm for current sharing and voltage regulation in DC microgrids. *IEEE Trans. Smart Grid* **2020**, *11*, 577–589. [CrossRef]
13. Peng, J.; Fan, B.; Xu, H.; Liu, W. Discrete-time self-triggered control of DC microgrids with data dropouts and communication delays. *IEEE Trans. Smart Grid* **2020**, *11*, 4626–4636. [CrossRef]
14. Zhang, N.; Sun, Q.; Yang, L.; Li, Y. Event-triggered distributed hybrid control scheme for the Integrated Energy System. *IEEE Trans. Ind. Inform.* **2022**, *18*, 835–846. [CrossRef]
15. Cucuzzella, M.; Trip, S.; De Persis, C.; Cheng, X.; Ferrara, A.; van der Schaft, A. A robust consensus algorithm for current sharing and voltage regulation in DC microgrids. *IEEE Trans. Control. Syst. Technol.* **2019**, *27*, 1583–1595. [CrossRef]
16. Wang, B.; Wang, Y.; Xu, Y.; Zhang, X.; Gooi, H.B.; Ukil, A.; Tan, X. Consensus-based control of hybrid energy storage system with a cascaded multiport converter in DC microgrids. *IEEE Trans. Sustain. Energy* **2020**, *11*, 2356–2366. [CrossRef]

17. Lin, P.; Zhao, T.; Wang, B.; Wang, Y.; Wang, P. A semi-consensus strategy toward multi-functional hybrid energy storage system in DC microgrids. *IEEE Trans. Energy Convers.* **2020**, *35*, 336–346. [CrossRef]
18. Li, F.; Lin, Z.; Qian, Z.; Wu, J.; Jiang, W. A dual-window DC bus interacting method for DC microgrids hierarchical control scheme. *IEEE Trans. Sustain. Energy* **2020**, *11*, 652–661. [CrossRef]
19. Sun, J.; Lin, W.; Hong, M.; Loparo, K.A. Voltage Regulation of DC-microgrid with PV and Battery. *IEEE Trans. Smart Grid* **2020**, *11*, 4662–4675. [CrossRef]
20. Gamage, V.; Withana, N.; Silva, C.; Samarasinghe, R. Battery Energy Storage based approach for grid voltage regulation in renewable rich distribution networks. In Proceedings of the 2020 2nd IEEE International Conference on Industrial Electronics for Sustainable Energy Systems (IESES), Cagliari, Italy, 1–3 September 2020.
21. Chamana, M.; Jahanbakhsh, F.; Chowdhury, B.H.; Parkhideh, B. Dynamic ramp rate control for voltage regulation in distribution systems with high penetration photovoltaic power generations. In Proceedings of the 2014 IEEE PES General Meeting | Conference & Exposition, National Harbor, MD, USA, 27–31 July 2014.
22. Gong, B.; Cheng, S.; Qin, Y. Simple three-level neutral point voltage balance control strategy based on SVPWM. *Arch. Electr. Eng.* **2013**, *62*, 15–23. [CrossRef]
23. Hwang, J.G.; Lehn, P.W.; Winkelnkemper, M. Control of Grid Connected AC-DC converters with minimized DC link capacitance under unbalanced grid voltage condition. In Proceedings of the 2007 European Conference on Power Electronics and Applications, Aalborg, Denmark, 2–5 September 2007.
24. Zhang, W.; Li, X.; Du, C.; Wu, X.; Shen, G.; Xu, D. Study on neutral-point voltage balance of 3-level NPC inverter in 3-phase 4-wire system. In Proceedings of the 2nd International Symposium on Power Electronics for Distributed Generation Systems, Hefei, China, 16–18 June 2010.
25. Cha, D.-S.; Choi, J.-S.; Oh, S.-Y.; Ahn, H.-J.; Lim, Y.-C. Hot-swappable modular converter system control for heterogeneous batteries and ESS. *Energies* **2018**, *11*, 309. [CrossRef]